Medical Engineering and Physics 74 (2019) 65–72

Contents lists available at ScienceDirect

Medical Engineering and Physics

journal homepage: www.elsevier.com/locate/medengphy

Integration between volumetric change and strain for describing the global mechanical function of the left ventricle

Gianni Pedrizzetti[a,*], Radu Tanacli[b,c], Tomas Lapinskas[b,c,d], Luigino Zovatto[a], Burkert Pieske[b,c,e], Giovanni Tonti[f], Sebastian Kelle[b,d,e]

[a] Department of Engineering and Architecture, University of Trieste, Italy
[b] Department of Internal Medicine/Cardiology, German Heart Center Berlin, Berlin, Germany
[c] DZHK (German Centre for Cardiovascular Research), Partner Site Berlin, Germany
[d] Department of Cardiology, Medical Academy, Lithuanian University of Health Sciences, Kaunas, Lithuania
[e] Department of Internal Medicine/Cardiology, Charité Campus Virchow Clinic, Berlin, Germany
[f] Institute of Cardiology and Center of Excellence on Aging, "G. D'Annunzio" University of Chieti, Italy

ARTICLE INFO

Article history:
Received 30 April 2019
Revised 9 July 2019
Accepted 28 July 2019

Keywords:
Left ventricle
Systolic function
Ejection fraction
Global longitudinal strain
Global circumferential strain
Feature tracking
Deformation imaging

ABSTRACT

Introduction: Evaluations of left ventricular systolic function based on ejection fraction (EF) alone are unable to recognize impaired myocardial performance in some dysfunctional states, and strain parameters are often invoked for an improved description of cardiac contraction. A comprehensive framework integrating deformation measures with volumetric changes is therefore necessary.
Methods: This study presents a general mathematical background that confirms and generalizes a previously proposed framework relating volumetric changes and strain values. The model is then validated with 5450 data samples made of LV volume, global longitudinal strain (GLS) and global circumferential strain (GCS) from 109 heterogeneous subjects who underwent cardiac magnetic resonance imaging. The GCS was measured by either three short-axis slices or 3D LV geometry reconstructed from 3 long-axis slices.
Results: Results demonstrated the reliability of the relationship $EF = 1-(GLS+1)(GCS+1)^2$. Accuracy is higher (correlation coefficient $r = 0.997$) when GCS is obtained by 3D deformation, although it remains high ($r = 0.98$) when GCS is measured from short-axis slices. However, the latter may underestimate (about 10% in relative terms) the circumferential deformation due to through-plane motion.
Conclusions: The accuracy of this relationship permits a unitary description of LV systolic function in terms of both EF and global strain values by its position on the strain plane (GLS, GCS). This also allows to monitor pathologic or healing changes, as a consequence of exercise, drugs, surgery or other therapeutic options, as trajectories on that plane.

1. Introduction

Volumetric measurements of the left ventricle (LV) represent the main clinical reference for describing its contractile function. In particular, the ejection fraction (EF), defined as difference between end-diastolic LV volume, V_{ED}, and end-systolic LV volume, V_{ES}, normalized with the former, was found to be a predictive factor of numerous adverse clinical outcomes including heart failure (HF) [1]. Nevertheless, the description of LV systolic function based on EF alone is certainly incomplete and several HF states can develop in association with a preserved EF [2–4].

Since a few years, the advent of deformation imaging in echocardiography and cardiac magnetic resonance (CMR) allowed to an improved understanding of LV mechanical function, described not only in terms of volume change but also of myocardial deformation. This is typically evaluated in terms of global longitudinal strain (GLS), that describes the base-apex shortening, and global circumferential strain (GCS), for the reduction of circumference (or mean diameter) in the cross-section. Based on these, cardiac dysfunctions were also characterized in terms of alterations in the strain pattern [5]. However, EF and strain were mainly considered as separate information in the clinical context [6,7], although the need of an integrated assessment was clearly recognized [8].

Recently, two studies introduced a new framework to integrate the relative volumetric change with strain measurements in a unitary picture of LV contraction [9,10]. These studies were based on

* Corresponding author.
E-mail address: giannip@dia.units.it (G. Pedrizzetti).

https://doi.org/10.1016/j.medengphy.2019.07.016
1350-4533/

the existence of a mathematical relationship between EF, GLS and GCS. Such a relationship was derived in [9] for the special case of a prolate spheroid geometry and was validated in 100 echocardiographic [9] and 200 CMR [10] recordings of patients with different pathologies demonstrating a very good accuracy in general.

These results are expected to have an important impact on future descriptions of cardiac function in the clinical settings. It is therefore important to provide further mathematical background and define the possibly involved approximations. Although LV volumes and longitudinal strain are defined in a consistent manner in different imaging modalities, the quantification of circumferential strain may present significant differences in different contexts. Ideally, GCS is measured on slices that span the LV length from base to apex during its base-to-apex shortening. This evaluation can be achieved, in principle, by three-dimensional (3D) imaging. More commonly, however, GCS is measured in two-dimensional (2D) images takes on transversal (short-axis, SAX) slices at fixed position in space and results can present a systematic difference [11].

The present study aims to strengthen the approach introduced by Stokke et al. [9] and Pedrizzetti and co-workers [10] by

(i) Presenting a general mathematical background of the relationship between volumetric changes and strain values.
(ii) Provide further validation, using multiplane CMR, comparing results based on GCS measured by multiple 2D SAX and by 3D geometry.

2. Materials and methods

2.1. Mathematical relationship between relative volumetric changes and strain

Consider a generic LV whose long-axis is H and its mean transversal diameter is D; the LV volume can be generally expressed as $V = cHD^2$, where c is a dimensionless coefficient which depends on the specific shape of the LV (for example, in the case of half a prolate spheroid, $c = \frac{\pi}{6}$). The EF can then expressed in general

$$\mathrm{EF} = 1 - \frac{V_{\mathrm{ES}}}{V_{\mathrm{ED}}} = 1 - \frac{c_{\mathrm{ES}}}{c_{\mathrm{ED}}} \frac{H_{\mathrm{ES}}}{H_{\mathrm{ED}}} \frac{D_{\mathrm{ES}}^2}{D_{\mathrm{ED}}^2}. \tag{1}$$

where the subscripts indicate that the values are relative to the end-systolic (ES) and end-diastolic (ED) instants as sketched in Fig. 1(A).

Following the same dimensional argument, the LV endocardial longitudinal length can be expressed in general proportional to the LV length, aH, and the circumference proportional to the diameter, bD. Using these, assuming the undeformed configuration at ED, the ES values of GLS and GCS can be expressed

$$\mathrm{GLS} = \frac{a_{\mathrm{ES}}}{a_{\mathrm{ED}}} \frac{H_{\mathrm{ES}}}{H_{\mathrm{ED}}} - 1; \qquad \mathrm{GCS} = \frac{b_{\mathrm{ES}}}{b_{\mathrm{ED}}} \frac{D_{\mathrm{ES}}}{D_{\mathrm{ED}}} - 1; \tag{2}$$

where, as before, the dimensionless coefficients a and b depend on the specific LV shape. For example, in the case of half a prolate spheroid, $a = 2E(1 - \frac{1}{4}\frac{D^2}{H^2})$ (where E is the Legendre complete elliptic integral of second kind) that is weakly varying with the axis ratio (for reference when $\frac{H}{D} = 2$ we have $a = 2.145$ and the limiting value for $H \gg D$ is $a = 2$), and $b = \frac{\pi}{2}$. In (2) we assumed that GLS and GCS represent a measure of the relative change in the average LV length and diameter, respectively. This corresponds to assuming a certain regularity (not necessarily uniformity) in the deforming shape and that measurement are representative for the entire LV.

The ratio between LV long-axis lengths ($\frac{H_{\mathrm{ES}}}{H_{\mathrm{ED}}}$) and between LV diameters ($\frac{D_{\mathrm{ES}}}{D_{\mathrm{ED}}}$) can be extracted from (2) and inserted into (1). This provides the following mathematical relationship expressing EF as a function of end-systolic GLS and GCS

$$\mathrm{EF} = 1 - \kappa\,(\mathrm{GLS} + 1)(\mathrm{GCS} + 1)^2; \tag{3}$$

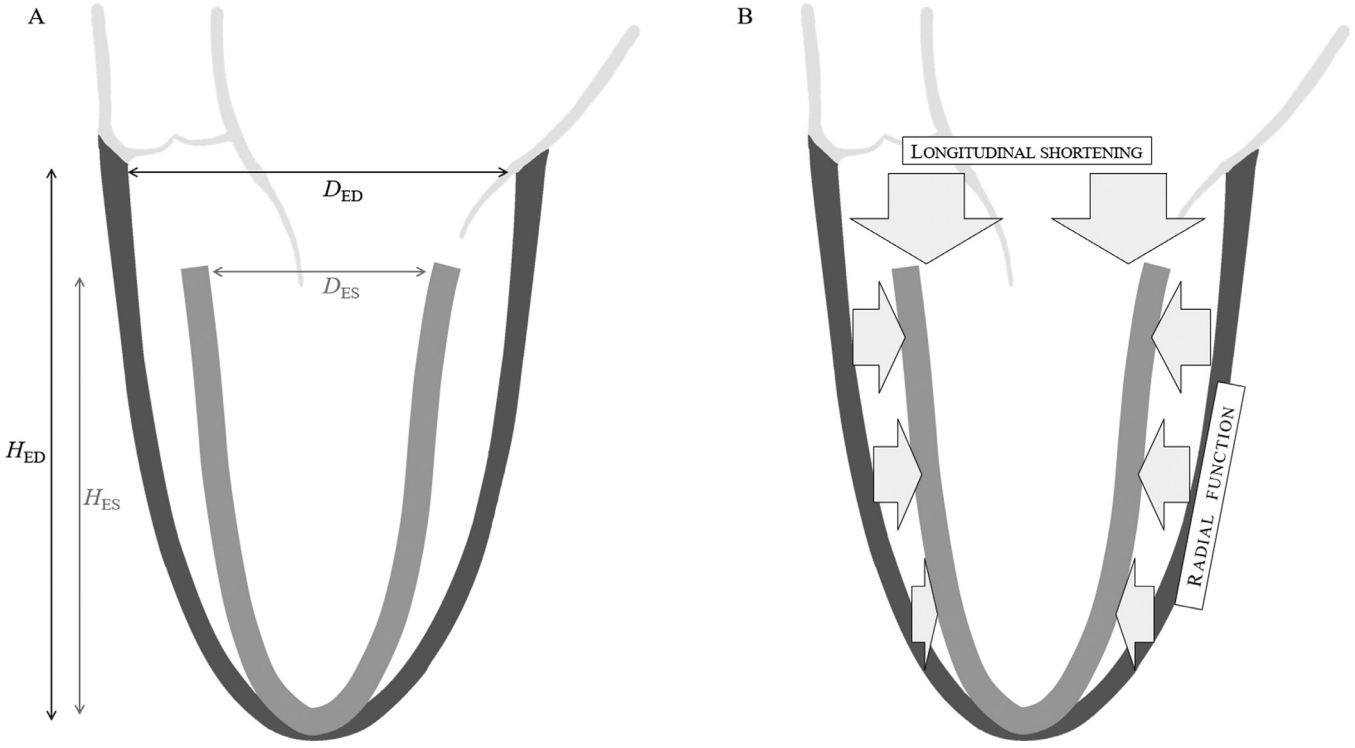

Fig. 1. Sketch of left ventricular (LV) contraction: (A) the reduction of size from end-diastole (ED) to end- systole (ES) can be represented with a reduction of LV height H and diameter D; (B) the global reduction of the geometry can be separated in a longitudinal shortening and a radial function that gives the reduction of the transversal section.

which is formally exact although the constant $\kappa = \frac{c_{ES}}{c_{ED}} \frac{a_{ED}}{a_{ES}} \frac{b_{ED}^2}{b_{ES}^2}$ depends on the change in LV shape from ED to ES. It can be further noticed that this constant is a ratio between coefficients that are expected to change similarly along the cardiac cycle (constant c is likely to be nearly proportional to ab^2); making it very weakly dependent on the LV shape. Therefore, a value substantially different from $\kappa = 1$ can occur only in presence of extremely large alteration of the LV geometry during the contraction. To give a quantification, if the ratio $\frac{H}{D}$ changes as much as from 2 to 4, between diastole and systole, the value of κ differs less than 5% to from unity. Therefore, the constant κ can be assumed with good confidence equal to unity, unless the changes in LV shape during the heartbeat are dramatically extreme, like in presence of a large apical aneurysm or other visually evident pathology that would dominate the clinical focus.

This result sets out the mathematical ground for differentiating the contributions to cardiac contraction that, as shown in Fig. 1(b), is imputable to longitudinal shortening quantified by the GLS, and to the radial function quantified by the GCS, as

$$\mathrm{EF} = 1 - (\mathrm{GLS} + 1)(\mathrm{GCS} + 1)^2. \tag{4}$$

Relationship (4), which has no unknown or adjustable coefficients, permits to estimate EF once the values of GLS and GCS are known. It allows drawing curves with constant EF on the GLS-GCS plane (the strain plane), as shown in Fig. 2. Different points belonging to a curve EF = constant represent contraction patterns with the same EF and different relative contribution between

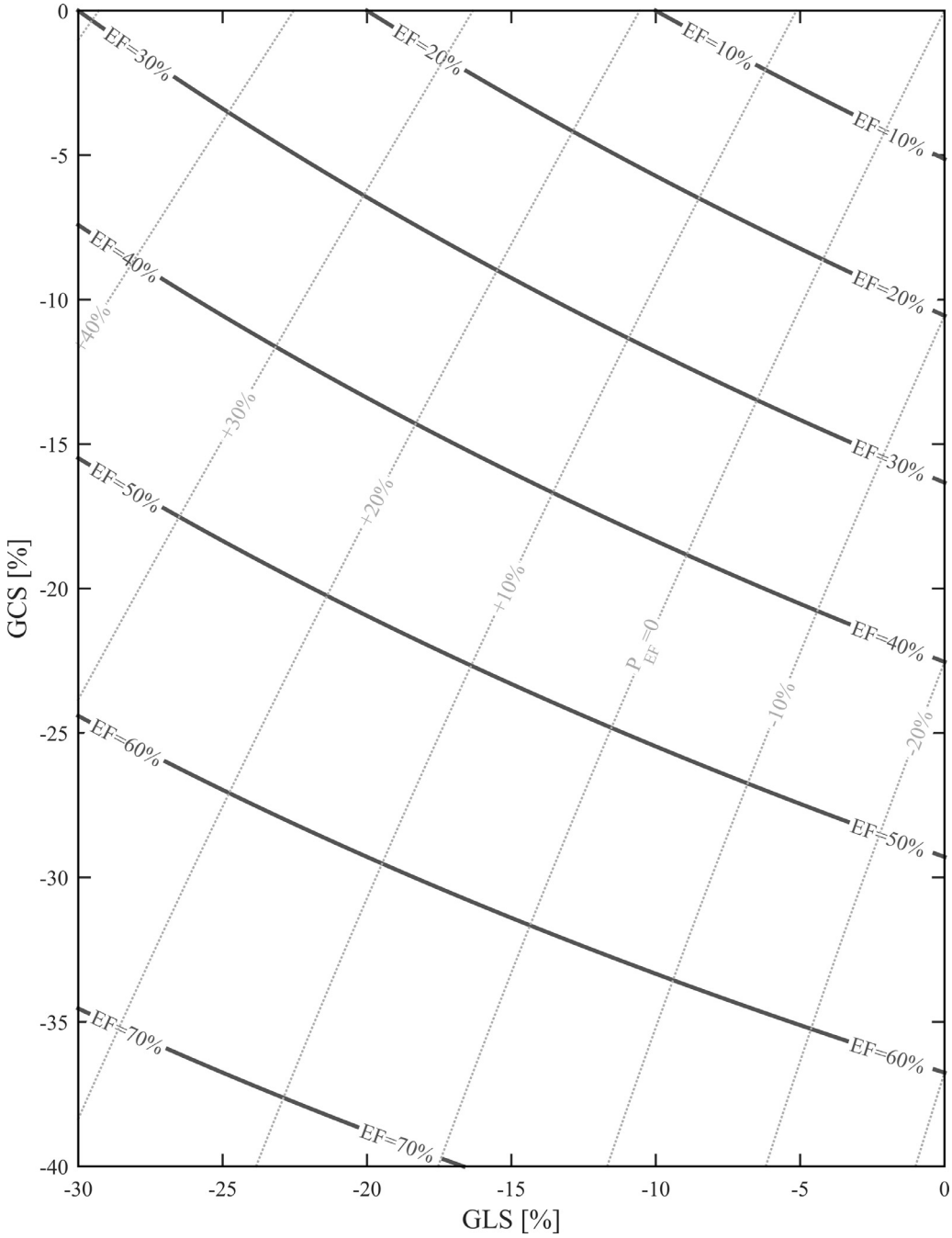

Fig. 2. Graphical representation of the relationship between ejection fraction (EF), global longitudinal strain (GLS) and global circumferential strain (GCS). That relationship permits to drawing curves at constant EF on the GLS–GCS plane (thick line); the curves orthogonal to these (thin dotted line) are identified by the parameter P_{EF}.

longitudinal and radial function. The same equation can be obtained from the model previously presented by Stokke and coworkers [9] for the specific case of a prolate spheroid geometry, taking the strain measured at the endocardium.

Looking at Fig. 2, it may be useful to construct a parameter that is strictly orthogonal to EF made by a proper combination of GLS and GCS that varies along curves of preserved EF and does not vary when moving perpendicular to those. This parameter can obtained by computing the gradient of EF with respect to GLS and GCS in (4) and setting it to zero

$$\frac{d\mathrm{GLS}}{(\mathrm{GLS}+1)} = -2\frac{d\mathrm{GCS}}{(\mathrm{GCS}+1)}. \tag{5}$$

The differential relation (5) can be easily integrated to get the parameter *perpendicular to* EF, which varies along curves at constant EF

$$P_{\mathrm{EF}} = \frac{1}{2} + \frac{1}{2}(\mathrm{GCS}+1)^2 - (\mathrm{GLS}+1)^2; \tag{6}$$

where the integration constant was arbitrarily selected to give $P_{\mathrm{EF}} = 0$ when both strains are zero. As shown in Fig. 2, variation of P_{EF} correspond to changes in both GLS and GCS such that EF is preserved.

It is useful to remark that the relationship (4) was obtained from a general argument applied to the ES instant. However, the same arguments can be applied to any instant t during the cardiac cycle. Therefore, relationship (4) can also be extended to one

$$\frac{V_{\mathrm{ED}} - V(t)}{V_{\mathrm{ED}}} = 1 - (\mathrm{GLS}(t)+1)(\mathrm{GCS}(t)+1)^2. \tag{7}$$

between the relative volumetric changes and the values of global strain at any instants during the heartbeat. On the clinical side, the interest of the extended relationship (7) is certainly lower; however, this formula permits to extend the validation of formula (4) and (7) to all the time points during the heartbeat thus increasing of over one order of magnitude the validation sample.

2.2. Sample population data

We retrospectively enrolled 109 subjects into the study from two centers: 68 patients and 41 matched healthy volunteers from studies in heart failure and deformation imaging. We included patients with a clinical diagnosis of HF supported by CMR, echocardiographic and laboratory tests as recommended by the most recent ESC guidelines [12]. Of these, 29 had preserved ejection fraction but were symptomatic and had diastolic dysfunction on echocardiogram and/or abnormal blood levels of NT-proBNP. The rest of 39 had an EF below the threshold of normality (assumed EF = 55%). As the purpose of our study was to establish the relation between myocardial strain and EF we sought to include patients with a variety of EF impairment. Importantly, of these 39 patients, 19 have HF but only mid-range reduced EF, a recently described subgroup of patients in which the relationship between intrinsic contractility and cardiac output is under debate and insufficiently characterized. Comorbidities such as CAD, HTN, diabetes and hypercholesterolemia were equally distributed between these subgroups of HF patients. All patients gave written informed consent. The study protocols were approved by the local Ethics Committees and complied with the Declaration of Helsinki. The main clinical parameters and mean volumetric and deformation characteristics are reported in Table 1.

All participants underwent standard CMR on a 1.5 Tesla clinical MRI scanner (Achieva, Philips Heathcare, Best, the Netherlands). Cine images were acquired using ECG-gated balanced steady state free precession (bSSFP) sequence with multiple breathholds at end-expiration in three LV long-axis (two-, three- and four-chamber) planes and a stack of short-axis slices covering the entire LV with a resolution (voxel size) $1.8 \times 1.7 \times 8.0\,\mathrm{mm}^3$. All cine images were analyzed offline by CMR Level 3 certified investigators using Medis Suite, version 3.0 (Medis BV, Leiden, The Netherlands) in compliance with a recent consensus document for quantification of LV function [13].

The cine images were also used to calculate myocardial strain using dedicated software (QStrain 1.3.0.79, Medis BV, Leiden, The Netherlands). LV endocardial borders were contoured in three SAX slices (basal, mid-ventricular, and apical) for computing the GCS (that we call $\mathrm{GCS_{SAX}}$) and in three long-axis planes (two-, three- and four-chamber) for GLS as the average of the values obtained from each slice. The three long-axis slices are also used to reconstruct the 3D LV shape that is used for a second computation of GCS ($\mathrm{GCS_{3D}}$) as the average of circumferential contraction from base to apex. The main difference between the $\mathrm{GCS_{SAX}}$ and $\mathrm{GCS_{3D}}$ is that the former is evaluated on 3 slices that are fixed in space and may be affected by cross-plane motion during LV shortening, whereas the latter uses a fixed number of slices from base to apex along the varying LV length.

The CMR cines were composed of a variable number of phases ranging from 25 to 50 in SAX recordings (25 phase in 11%, 40 phases in 21%, 50 phases in 68%) and from 40 to 50 in long-axis (40 phases in 31%, 50 phases in 69%). All the time courses of LV volume and strain curves were resampled to 50 time instants during the cardiac cycle. This resulted in 5450 (50×109) samples used in the validation of formula (7).

Table 1
Characteristics of the sample population (Volunteers did not undergo to echocardiographic examination and blood sampling to measure BNP).

	Volunteers ($n = 41$)	Patients ($n = 68$)	Total ($n = 109$)
Age	44.9 ± 6.9	67.2 ± 8.2	58.8 ± 13.3
Male subjects	22 (54%)	37 (54%)	59 (54%)
E/e' (echo)		11.8 ± 4.4	
LV EF [%] (echo)		52.1 ± 11.4	
NT-proBNP [pg/mL]		996 ± 1421	
Heart Rate	60.2 ± 9.4	65.8 ± 8.5	63.7 ± 9.3
LA surface [$\mathrm{cm^2}$]	21.4 ± 3.2	26.1 ± 4.1	24.3 ± 4.4
RA surface [$\mathrm{cm^2}$]	22.8 ± 4.5	22.1 ± 4.7	22.4 ± 4.6
LVMi [$\mathrm{g/m^2}$]	44.8 ± 7.1	119.0 ± 58.2	91.1 ± 58.6
LV V_{ED} [$\mathrm{cm^3}$]	145 ± 30	186 ± 66	171 ± 59
LV V_{ES} [$\mathrm{cm^3}$]	52 ± 16	97 ± 58	80 ± 52
LV EF [%]	64.3 ± 6.6	51.6 ± 13.9	56.4 ± 13.2
GLS [%]	−23.4 ± 2.9	−17.0 ± 5.7	−19.4 ± 5.7
$\mathrm{GCS_{3D}}$ [%]	−33.7 ± 6.2	−25.6 ± 10.3	−28.6 ± 9.8
$\mathrm{GCS_{SAX}}$ [%]	−30.5 ± 6.0	−23.1 ± 11.0	−25.9 ± 10.1

Values are reported as mean ± standard deviation.

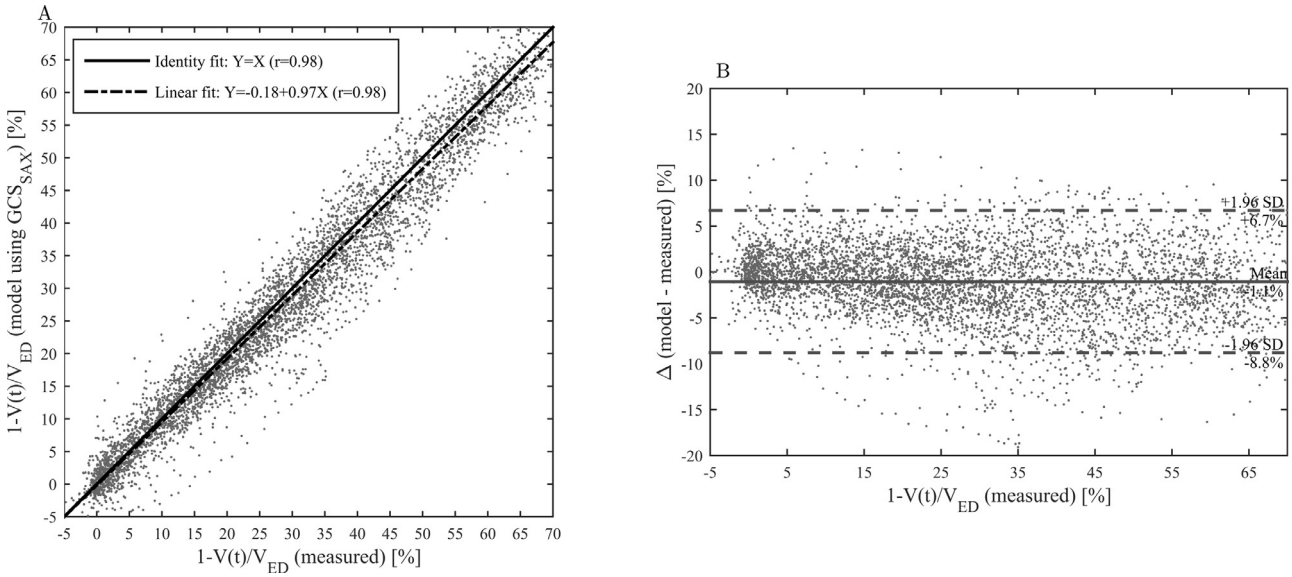

Fig. 3. Correlation between the measured values of $\frac{V_{ED}-V(t)}{V_{ED}}$ and those computed by the model (7) using the global longitudinal strain and the global circumferential strain values at the same instants. The latter is measured from short-axis slices. (A) Correlation graph; (B) Bland–Altman analysis.

3. Results

3.1. Model validation using GCS_{sax}

The volumetric change obtained from measurements is first compared with the same obtained from the model (7) using the GCS measured in SAX slices. Fig. 3(A) shows that the model results present a very good correlation, with a correlation coefficient $r = 0.98$ for the complete linear fit. As the model is theoretically aimed to be equal to the measurement, we also evaluate the correlation of an identity relationship which results in a similar correlation coefficient $r = 0.98$. The Bland–Altman analysis of the difference between estimated and measured values, reported in Fig. 3(B), shows a small bias $= -1.1\%$ with a standard deviation of 3.95% and no evident systematic trend.

These figures are in line with previous results [9,10], which reported a correlation $r = 0.95$ for comparisons performed with the end-systolic values only. The present results therefore confirm the overall reliability of the model (4) or (7). Discrepancies can be imputable to measurement errors although the variability is some higher than commonly expected in clinical measurements of EF that is around or below 5% [14]. This apparently suggests that the variability of the EF evaluated from the model can be slightly larger than the EF directly measured.

3.2. Comparison between GCS_{sax} and GCS_{3d}

The GCS computed on fixed SAX slices is expected to differ from the GCS computed on moving slices covering the LV from based to apex. The correlation analysis between the two measurements of GCS, reported in Fig. 4(A), evidences a good correlation of the $GCS_{3D} = GCS_{SAX}$ assumption ($r = 0.96$); however, it also evidences the systematic underestimation of circumferential strain measured in SAX slices, with a best fit $GCS_{3D} = 1.09 \times GCS_{SAX}$ ($r = 0.97$). This

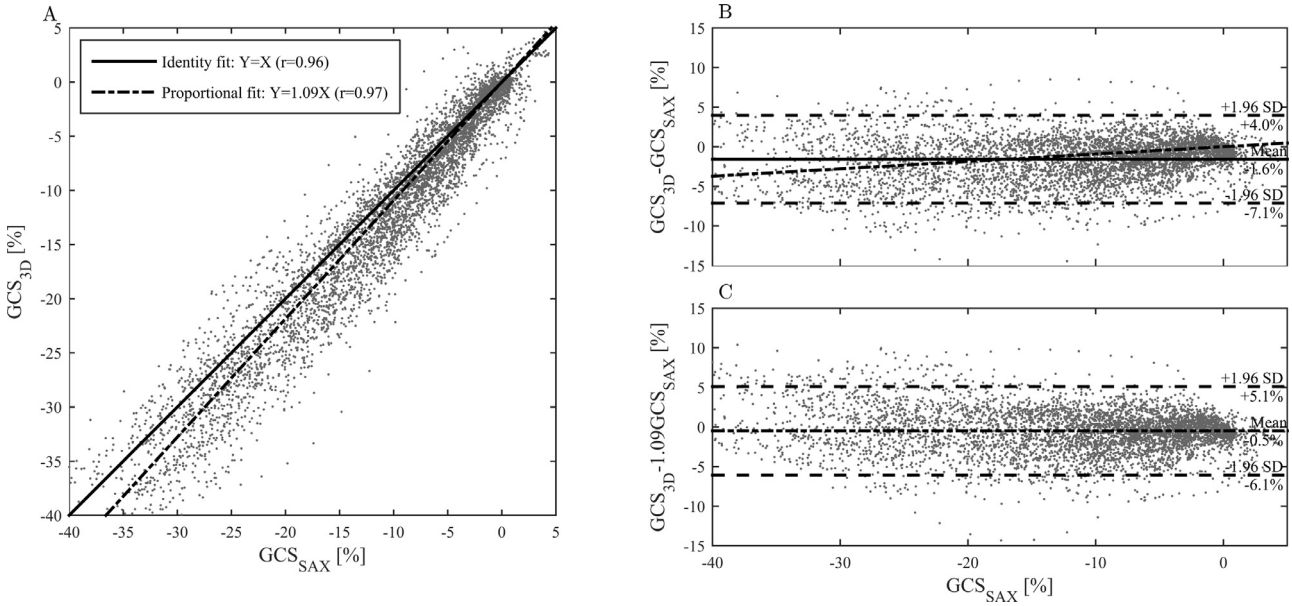

Fig. 4. Correlation between the global circumferential strain measured from short-axis slices (GCS_{SAX}) and the same measured from 3D deformation measured (GCS_{3D}). (A) Correlation graph; (B) Bland–Altman analysis; (C) Bland–Altman analysis corrected for the best correlation.

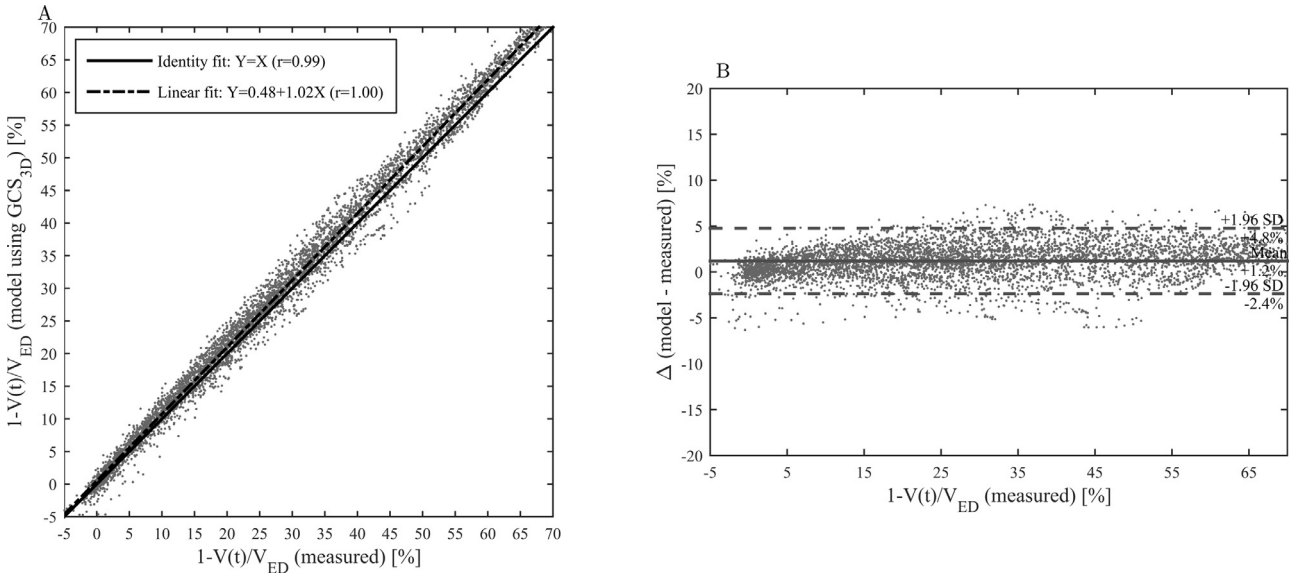

Fig. 5. Correlation between the measured values of $\frac{V_{ED}-V(t)}{V_{ED}}$ and those computed by the model (7) using the global longitudinal strain and the global circumferential strain values at the same instants. The latter is measured from 3D deformation reconstructed from long-axis slices. (A) Correlation graph; (B) Bland–Altman analysis.

becomes evident in the Bland–Altman analysis where the difference between the two, in Fig. 4(B), shows a systematic trend that disappears, in Fig. 4(C), when the difference is corrected by the underestimation factor.

The possible underestimation of GCS measured from SAX slices was previously reported in comparative studies of 2D echocardiography and CMR with 3D echocardiographic; in contrast, the same studies showed that GLS is comparable or slightly lower in 3D echocardiography due to the lower time resolution [11,15]. Indeed, the underestimation of GCS_{SAX} is imputable to the through-plane motion: during the systole, while the LV contracts radially, the base moves toward the apex; therefore, a transversal slice taken at a fixed spatial position displays a portion of the LV that becomes more basal as the contraction proceeds, and a more basal slice is a bit wider thus shows an apparently less contracting tissue. In addition to the through plane effect, the SAX slices do not cover very well the apex where circumferential strain tends to be higher, whereas the apical part is well covered in a 3D LV model.

3.3. Model validation using GCS_{3d}

The measured volumetric changes are now compared with the same obtained from the model (7) using the GCS obtained from 3D LV deformation. Fig. 5(A) shows that the model result presents an excellent correlation both for a linear fit ($r = 0.997$) and for the identity relationship ($r = 0.995$). The Bland-Altman analysis, in Fig. 5(B), shows a very small bias=1.2%, small standard deviation 1.84%, and no systematic trend. The comparison between Figs. 5 and 3 evidences the significant improvement in the usage of the 3D GCS where discrepancies are smaller than the variability expected in clinical measurements.

This improvement is not surprising because both volume and strain measurements are obtained from the same 3D LV model and differences due to different image stacks are not present. On the other hand, this result confirms the theoretical reliability of the model (4) and (7).

3.4. Application to clinical data

The mathematical relationship (4) allows portraying in a graphical representation the curves with constant EF in the plane described by GLS (x-coordinate) and GCS (y-coordinate). Each subject is represented by a point in this plane identified by its coordinates, the GLS and GCS values, which correspond to a value of EF given by Eq. (4). This representation is provided in Fig. 6 for all the subjects included in this study. The same graph includes the curve $EF = -3GLS$ as a reference, which is considered a typical relationship holding in normal LV geometries.

The volunteers are all distributed above the level EF = 55% (with one exception), whereas the patients – presenting heterogeneous pathologies – spread across different levels of EF. They also extend toward reduced levels of the parameter P_{EF}, that represents changes in the contraction pattern not associated with changes in EF. These examples were shown with the aim of introducing the graphical representation with real data. However, pursuing clinical results is out of the scope of this study and subjects were randomly chosen with the purpose of model validation only.

This graphical representation permits the integration of information about EF with measures of deformation. It contains curves at constant EF, thus demonstrating that a same EF can be obtained with different pairs of GLS and GCS corresponding to different patterns of contraction. Thus, when EF is preserved, a reduction of GLS must be accompanied by a corresponding increase of GCS and vice versa; values that can be calculated numerically by Eq. (4).

4. Discussion

The validation results demonstrate the accuracy of the model in predicting EF based on global longitudinal and circumferential strain values. The latter is best estimated by 3D deformation whereas measurement based on short-axis slices may be underestimated of about 9% in relative terms. The mathematical model is based on geometrical principles and it is purely predictive, in the sense that it contains no adjustable coefficient. Its accuracy should not be confused with the good linear correlations between EF and individual global strain values reported elsewhere in the literature [9,16,17]. Linear regressions have no theoretical background in support, they are a statistical data-fit with adjustable coefficients that are optimized on the specific dataset and have no general validity.

CMR is the current reference standard for assessing EF. Due to its superior temporal resolution and more solid validation in vivo, echocardiography was shown to be an appropriate technique to

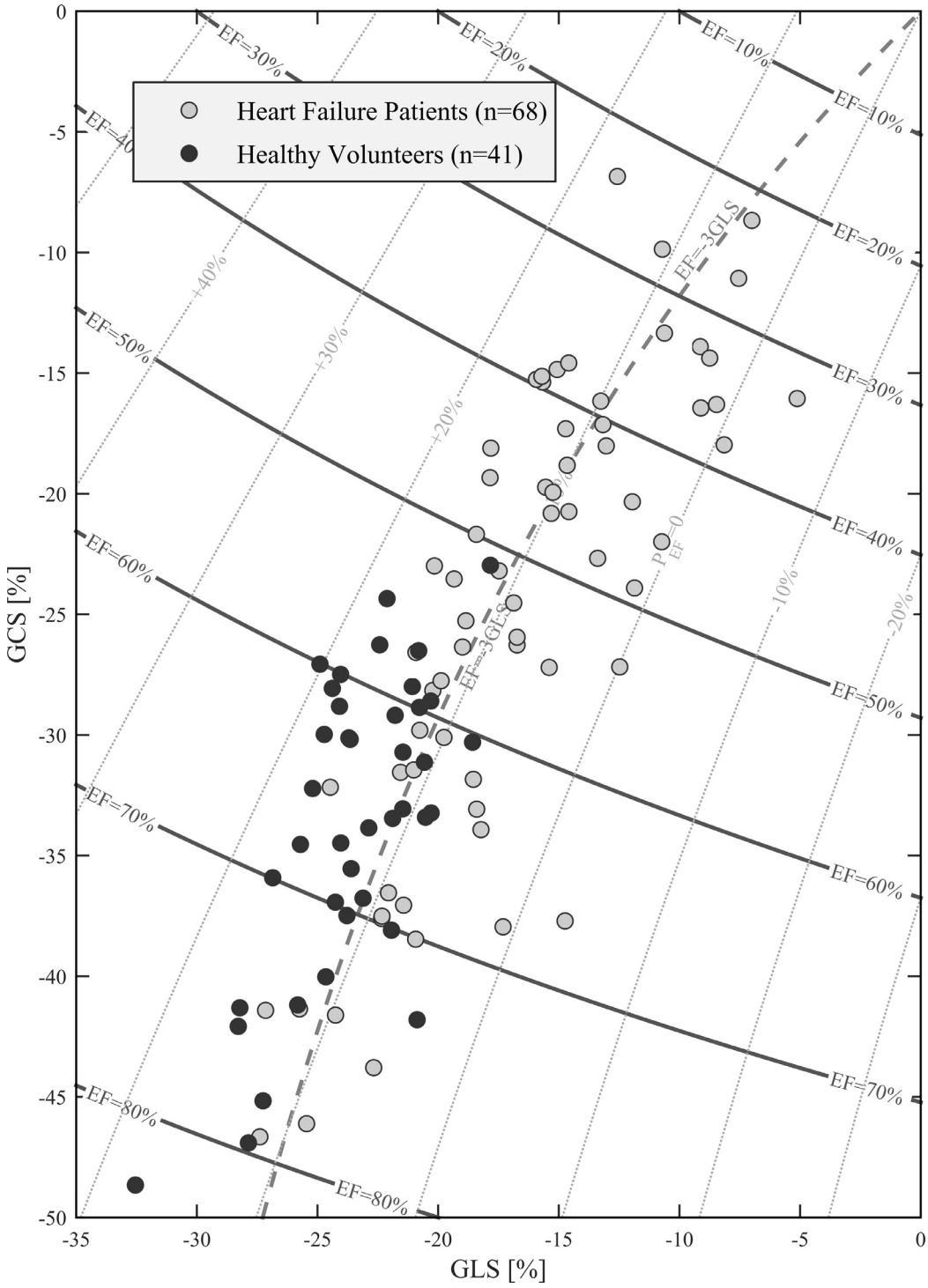

Fig. 6. End-systolic deformation parameters reported in the GLS–GCS plane for all the population included in this study. The continuous thick lines are the curves at constant EF as given by the theoretical formula, point lines are perpendicular to these, at constant P_{EF}; gray dashed line represents the empirical relationship EF = −3GLS.

assess GCS and GLS. Feature tracking in CMR permits to assess strain with good reproducibility and very good agreement with echocardiographic values. We therefore believe that echo-derived strain parameters would be in line with our findings. Indeed our findings are in good agreement with a similar analysis performed with strain and volumetric parameters evaluated by echocardiography [9].

Studies about cardiac deformation can differ in the choice of the layer within the myocardium where strain is computed. The study that introduced the first version of the mathematical model used the strain evaluated at 33% of the thickness from the endocardium [9]; that approach required the introduction of two additional dimensional parameters in the model (myocardial thickness and LV diameter) and two numerical coefficients. In this study we chose to use strain at the endocardial level; this choice removes these additional dependencies and allows a substantial simplification of the model with a direct relationship between EF and strain. Clinical recommendations suggest that strain measurement should be endocardial, midline, or full wall [18]; while technical considerations suggest that evaluations are most effective around

endocardial borders which offer a more distinct interface with the cavity [19]. In any case it should be underlined that endocardial strain represents the ultimate results of myocardial contraction, whose function is that of reducing the cavity size.

The confidence on the relationship (4) also allows a simplification of clinical procedures. Commonly, measurements in deformation imaging focus on one strain value, typically GLS (sometime GCS in CMR). Application of this relationship permits to recover the value of GCS from EF and GLS (or GLS from EF and GCS) without the need of its direct measurement (the supplementary worksheet shows the placement of a measurement pair on the strain plane). Alternatively, when the three parameters are independently measured, the same relationship can be used as a check for the consistency of the results.

The systolic function is since ever fundamentally described by EF. However, in presence of numerous dysfunctions, e.g. pressure overload hypertrophy, EF might overestimate myocardial function inducing erroneous deductions about of the real mechanical performance of the LV. The position on the strain plane, provides a more comprehensive identification of cardiac performance based on the integration of myocardial deformation parameters (GLS, GCS) with EF. This can be useful not only during diagnosis, but especially for tracking progresses in cardiac performance during time, following progressive or acute therapeutic intervention, e.g. exercise, cardiotoxic drugs, surgery, that can be represented as healing or pathologic trajectories on the strain plane; the supplementary worksheet is a simple tool for representing a series of such measurements (EF and GLS or GCS) on that plane.

5. Conclusion

The mathematical ground of a relationship between EF and endocardial global strain (GLS and GCS) was presented. The relationship was validated demonstrating a high reliability, especially when GCS is measured from LV 3D deformation, because measurement based on short-axis slices may present a small underestimation due to through-plane motion. The rigorous geometric grounds and the general validity make this model a useful tool for a more complete cardiac assessments, demonstrating the relationship between EF and GLS, GCS and that these parameters represent different aspects of the same phenomenon and should not be considered separately.

Declaration of Competing Interest

GP and GT are shareholders of a company (AMID SRL, Sulmona, Italy) that has a commercial agreement with companies for development of software for deformation imaging in cardiology. SK received research support from Philips Healthcare. There are no other known conflicts of interest associated with this study and there has been no significant financial support for this work that could have influenced the results. GP and LZ were partly supported by Italian Ministry of Education and Research under project PRIN 2017A889FP.

Supplementary materials

Supplementary material associated with this article can be found, in the online version, at doi:10.1016/j.medengphy.2019.07.016.

References

[1] Yeboah J, Rodriguez CJ, Stacey B, Lima JA, Liu S, Carr JJ, et al. Prognosis of individuals with asymptomatic left ventricular systolic dysfunction in the multi-ethnic study of atherosclerosis (MESA). Circulation 2012;126:2713–19. doi:10.1161/CIRCULATIONAHA.112.112201.

[2] Edvardsen T, Helle-Valle T, Smiseth OA. Systolic dysfunction in heart failure with normal ejection fraction: speckle-tracking echocardiography. Prog Cardiovasc Dis 2006;49:207–14. doi:10.1016/j.pcad.2006.08.008.

[3] Omar AMS, Bansal M, Sengupta PP. Advances in echocardiographic imaging in heart failure with reduced and preserved ejection fraction. Circ Res 2016;119:357–74. doi:10.1161/CIRCRESAHA.116.309128.

[4] Sengupta PP, Narula J. Reclassifying heart failure: predominantly subendocardial, subepicardial, and transmural. Heart Fail Clin 2008;4:379–82. doi:10.1016/j.hfc.2008.03.013.

[5] Claus P, Omar AMS, Pedrizzetti G, Sengupta PP, Nagel E. Tissue tracking technology for assessing cardiac mechanics: principles, normal values, and clinical applications. JACC Cardiovasc Imaging 2015;8:1444–60. doi:10.1016/j.jcmg.2015.11.001.

[6] Krishnasamy R, Isbel NM, Hawley CM, Pascoe EM, Burrage M, Leano R, et al. Left ventricular global longitudinal strain (GLS) is a superior predictor of all-cause and cardiovascular mortality when compared to ejection fraction in advanced chronic kidney disease. PLoS One 2015;10:1–15. doi:10.1371/journal.pone.0127044.

[7] Kraigher-Krainer E, Shah AM, Gupta DK, Santos A, Claggett B, Pieske B, et al. Impaired systolic function by strain imaging in heart failure with preserved ejection fraction. J Am Coll Cardiol 2014;63:447–56. doi:10.1016/j.jacc.2013.09.052.

[8] Potter E, Marwick TH. Assessment of left ventricular function by echocardiography: the case for routinely adding global longitudinal strain to ejection fraction. JACC Cardiovasc Imaging 2018;11:260–74. doi:10.1016/j.jcmg.2017.11.017.

[9] Stokke TM, Hasselberg NE, Smedsrud MK, Sarvari SI, Haugaa KH, Smiseth OA, et al. Geometry as a confounder when assessing ventricular systolic function: comparison between ejection fraction and strain. J Am Coll Cardiol 2017;70:942–54. doi:10.1016/j.jacc.2017.06.046.

[10] Pedrizzetti G, Lapinskas T, Tonti G, Stoiber L, Zaliunas R, Pieske B, et al. The relationship between ejection fraction and strain permits a more accurate assessment of left ventricular systolic function. JACC Cardiovasc Imaging 2019. doi:10.1016/j.jcmg.2019.03.019.

[11] Saito K, Okura H, Watanabe N, Hayashida A, Obase K, Imai K, et al. Comprehensive evaluation of left ventricular strain using speckle tracking echocardiography in normal adults: comparison of three-dimensional and two-dimensional approaches. J Am Soc Echocardiogr 2009;22:1025–30.

[12] Ponikowski P, Voors AA, Anker SD, Bueno H, Cleland JGF, Coats AJS, et al. 2016 ESC guidelines for the diagnosis and treatment of acute and chronic heart failure. Eur Heart J 2016;37:2129–200. doi:10.1093/eurheartj/ehw128.

[13] Schulz-Menger J, Bluemke DA, Bremerich J, Flamm SD, Fogel MA, Friedrich MG, et al. Standardized image interpretation and post processing in cardiovascular magnetic resonance: society for cardiovascular magnetic resonance (SCMR) board of trustees task force on standardized post processing. J Cardiovasc Magn Reson 2013;15:1–19. doi:10.1186/1532-429X-15-35.

[14] Pellikka PA, She L, Holly TA, Lin G, Varadarajan P, Pai RG, et al. Variability in ejection fraction measured by echocardiography, gated single-photon emission computed tomography, and cardiac magnetic resonance in patients with coronary artery disease and left ventricular dysfunction. JAMA Netw Open 2018;1:e181456. doi:10.1001/jamanetworkopen.2018.1456.

[15] Obokata M, Nagata Y, Wu VCC, Kado Y, Kurabayashi M, Otsuji Y, et al. Direct comparison of cardiacmagnetic resonance feature tracking and 2D/3D echocardiography speckle tracking for evaluation of global left ventricular strain. Eur Heart J Cardiovasc Imaging 2016;17:525–32. doi:10.1093/ehjci/jev227.

[16] Onishi T, Saha SK, Delgado-Montero A, Ludwig DR, Onishi T, Schelbert EB, et al. Global longitudinal strain and global circumferential strain by speckle-tracking echocardiography and feature-tracking cardiac magnetic resonance imaging: comparison with left ventricular ejection fraction. J Am Soc Echocardiogr 2015;28:587–96. doi:10.1016/j.echo.2014.11.018.

[17] Pagourelias ED, Duchenne J, Mirea O, Vovas G, Van Cleemput J, Delforge M, et al. The relation of ejection fraction and global longitudinal strain in amyloidosis: implications for differential diagnosis. JACC Cardiovasc Imaging 2016;9:1358–9. doi:10.1016/j.jcmg.2015.11.013.

[18] Voigt J-U, Pedrizzetti G, Lysyansky P, Marwick TH, Houle H, Baumann R, et al. Definitions for a common standard for 2D speckle tracking echocardiography: consensus document of the EACVI/ASE/Industry task force to standardize deformation imaging. Eur Heart J Cardiovasc Imaging 2015;28:183–93. doi:10.1016/j.echo.2014.11.003.

[19] Pedrizzetti G, Claus P, Kilner PJ, Nagel E. Principles of cardiovascular magnetic resonance feature tracking and echocardiographic speckle tracking for informed clinical use. J Cardiovasc Magn Reson 2016;18:1–12. doi:10.1186/s12968-016-0269-7.